Received: 17 October 2024 | Revised: 08 December 2024 | Accepted: 04 January 2025

DOI: 10.5185/amlett.2025.011768

OPEN ACCESS

RESEARCH

Facile Synthesis of Disordered Graphitic Charcoal by Direct Pyrolysis of Mustard Oil Cake and Sugarcane Bagasse

Bidit Lamsal[1,2,3§], Deepshikha Karki[1,2,3§], Ramesh Puri[1,3], Kamal Prasad Sharma[4], Takahiro Maruyama[4], Rameshwar Adhikari[1,2,3]*

[1]Research Centre for Applied Science and Technology (RECAST), Tribhuvan University (TU), Kirtipur, 44618, Kathmandu, Nepal

[2]Central Department of Chemistry, TU, Kirtipur, 44618, Kathmandu, Nepal

[3]Nepal Polymer Institute (NPI), P. O. Box 24411, Kathmandu, Nepal

[4]Department of Applied Chemistry, Nanomaterials Research Centre, Meijo University, 1-501 Shigamaguchi, Tempaku, Nagoya, 468-8502, Japan

§ Equal contributing authors

***Corresponding author:**

E-mail:
rameshwar.adhikari@cdc.tu.edu.np
nepalpolymer@yahoo.com

ABSTRACT

Charcoal was prepared in a facile way using a muffle furnace by direct pyrolysis of mustard oil cake and sugarcane bagasse attempting inert gas-free high-temperature pyrolysis at 900 °C. The structure of the obtained product was analyzed by Raman spectroscopy, X-ray photoelectron spectroscopy (XPS), scanning electron microscopy (SEM) and Fourier transform infrared (FTIR) spectroscopy. The lack of long-range order in the prepared charcoal has been attested by the appearance of weak and broad 2D peaks in the Raman spectra. The diameter of the crystallites was found to be 3.66 nm (mustard oil cake) and 3.79 nm (sugarcane bagasse). The material was found to consist essentially of amorphous carbon with the presence of oxygen-containing functional groups. On analyzing the elemental composition by XPS, only carbon and oxygen atoms were observed. The charcoal was found to retain the layered morphology, organized in a sheet-like or flakes-like manner, of precursor lignocellulosic biomass. Charcoal with properties comparable to that obtained from the conventional method could be prepared in the absence of inert gas.

KEYWORDS

Charcoal; electron microscopy; spectroscopy; pyrolysis; oil cake.

HIGHLIGHTS

- Inert gas-free 900 °C pyrolysis of biomass on a normal muffle furnace was successful
- Charcoal with circa 4 nm crystallite size is obtained
- Layered morphology of biomass retained in the obtained charcoal

INTRODUCTION

Charcoal is a material that is produced by heating solid organic matter derived from either vegetable or animal sources in the absence of or limited supply of air at temperatures exceeding 300 °C [**1**]. This process is known as pyrolysis and the resulting material is called charcoal. The quality of charcoal produced depends on various factors, such as the composition of the substrate, rate of heating, pyrolysis temperature, flow of surrounding gaseous environment and the possibility of autocatalysis by volatile pyrolysis products [**2,3**].

Charcoal possesses various characteristics that are determined by the operating conditions and type of pyrolysis, such as density, mechanical resistance, humidity, fixed carbon content, ash content and volatile materials [**3–5**]. Carbon materials, including charcoal, can be classified based on their graphitic structure as graphitizable and non-graphitizable carbon. Graphitizable carbon is soft, has high density and can be converted to graphitic carbon by heating, whereas non-graphitizable carbon is hard, has low density and cannot be converted to graphitic carbon even at very high temperatures [**6–8**]. The amount of graphitic carbon in pyrolyzed biomass is generally a function of temperature where the graphitic domain increases with high-temperature pyrolysis [**9–12**]. However, the use of high temperatures in pyrolysis comes with a loss of yield, and therefore the temperature selection is a compromise that depends on the end use of the charcoal [**3,13**]. Carbon materials can be further classified based on their morphology, encompassing various forms such as glassy carbon, activated carbon, graphite, carbon fiber, carbon composite, graphite powder and carbon particles [**7,8**].

Numerous studies have been carried out on the synthesis of charcoal from various biomasses, such as tobacco, vine soot, banana pith, soybean oil cake, coffee, apple pulp, coir pith, oil cake/walnut, potato waste, and pulp tea [**14,15**]. During pyrolysis of biomass, inert gas, such as argon or nitrogen, is typically used to purge the system. The use of nitrogen, however, is accompanied by the incorporation of nitrogen groups in the charcoal which has been confirmed via Fourier Transform Infrared (FTIR) and X-ray Photoelectron Spectroscopy (XPS) [**16–18**]. The use of argon atmosphere solves the problem but for an added cost.

All things considered, the use of inert gas during high-temperature pyrolytic carbonization of biomass can result in nitrogen doping and an increase in the cost of synthesis, which may not always be desirable. Thus, attempts are being made to obtain carbonized biomass by direct pyrolysis in a muffle furnace [**3**].

The critical part of inert gas-free pyrolysis is the minimization of exposure of the sample to oxygen. The easiest method is to seal the material in an airtight container which may, however, add the risk of explosion due to pressure buildup. Using material that can sustain such high pressures is expensive and therefore nullifies the advantage of not using inert gases. Alternately sealing in porous material can slow oxygen diffusion but cannot entirely prevent it. Previous studies have shown that pyrolysis up to 400 °C is possible with sealed earthen pots but combustion was observed at higher temperatures [**8**]. Moreover, the sealing material should not contaminate the pyrolysis product. Here, we report inert gas-free pyrolysis of mustard oil cake and sugarcane bagasse in a muffle furnace with samples between copper plates which are then sealed by hammering. Hence, not only is the risk of explosion minimized but any possible contamination by oxides of copper can also be easily removed by mineral acids. It is worth stressing that no such contamination was observed (see section 3.1).

EXPERIMENTAL

Sample preparation

The overall preparation scheme of pyrolyzed carbon from mustard oil cake is shown in **Fig. 1** Mustard oil cake was purchased from Dang district while the sugarcane bagasse was collected from the local market, and the copper plate was purchased from Lalitpur.

Mustard oil cake and sugarcane bagasse each were washed, dried, and crushed into powder with the help of a laboratory grinder and then filtered through a 50 µm sieve. The fine powder that passed through the sieve of each sample was then placed in the middle of one of the copper plates (length: 3.4 cm, breadth: 3.3 cm, and thickness: 0.28 cm) onto which another copper plate was placed. The edges of the copper plate were folded to seal the whole setup by hammering.

The sealed setup was heated in a muffle furnace at a rate of 15 °C min^{-1}, held at 900 °C for an hour, and then allowed to cool in the air to ambient temperature from which black solid (charcoal) was obtained.

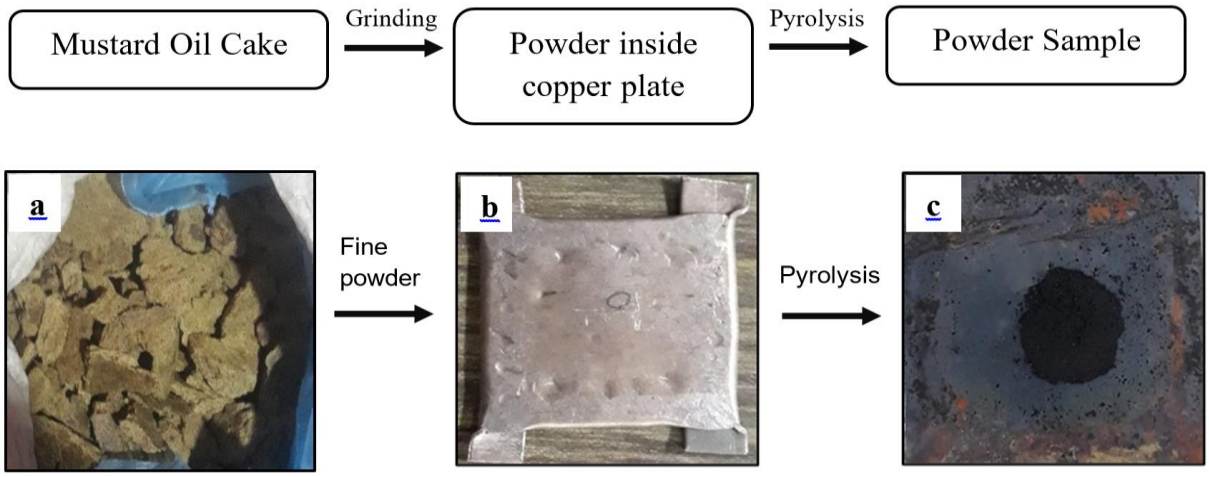

Fig. 1. Photographs showing different stages of preparation of charcoal from mustard oil cake (a) as obtained mustard oil cake (b) fine powder of mustard oil cake sealed in between the copper plate and (c) charcoal obtained by pyrolysis.

Characterization methods

Raman spectra were obtained by using a RAMAN force spectrometer, Nanophoton, Osaka, Japan to determine the graphitic phase and disorders in the sample. The excitation wavelengths used for Raman measurements were 532 nm, 671 nm and 785 nm. As the spectra from all three wavenumbers were similar, only the results from the excitation wavelength of 532 nm are elaborated in this report. Spectrum was obtained in the range of 102 cm^{-1} to 4333 cm^{-1} with wavenumber resolution 4 cm^{-1}. The samples were directly loaded on the spectrometer on a silica substrate. The baseline was corrected using asymmetric least square smoothing where the asymmetric factor was 0.001, the threshold was 0.01, the smoothing factor was 7

and iterations number 8. The D and 2D bands were fitted with the Lorentzian function and the G band was fitted with the Breit-Wigner Fano (BWF) function [**19**]. The peak area of D, G and 2D bands were obtained with the fitted curves and were denoted by I_D, $I_{G,}$ and I_{2D} respectively. The I_D/I_G ratio is used to determine the graphitic crystallinity in a sample [**20**].

X-ray photoelectron spectra were collected to determine the chemical composition of the samples. XPS was performed with a JPS-9200 instrument (JEOL, Tokyo, Japan) using Mg Kα (1253.6 eV) radiation. The samples were directly mounted without any treatment. The survey spectra were obtained in the range of 0 eV to 1000 eV with a resolution of 1 eV. Narrow spectra were obtained in the range of 274 eV to 304 eV for C1s transition and 522 eV to 542 eV for O1s transition with a resolution of 0.1 eV. The instrument-specific sensitivity factors for carbon and oxygen were 4.25 and 11.91, respectively. Tougaard baseline with a final height of 110 was used. The spectra were fitted with the Voigt function to determine the chemical state of carbon and oxygen.

Fourier Transform Infrared (FTIR) spectra of the sample were collected by using Shimadzu IR Tracer-100 spectrometer. The spectra were obtained within the range of 4000 cm^{-1} to 400 cm^{-1} and wave number resolution 2 cm^{-1} in Attenuated Total Reflectance (ATR) mode with powder placed on the specimen holder. The samples were directly analyzed without any pretreatment.

Scanning Electron Micrograph of the samples were collected using Hitachi S 3400 microscope at an accelerating voltage 5.00 KV. Samples were directly loaded on carbon tape without any treatment.

RESULTS AND DISCUSSION

Structural properties of samples

Fig. 2 shows the Raman spectra of mustard oil cake **Fig. 2(a)** and sugarcane bagasse **Fig. 2(b)** respectively with a laser of wavelength 532 nm along with a fitted curve. The spectrum of the sample from mustard oil cake shows three main bands with a maximum intensity peak located at 1354.40 cm^{-1}, 1598.78 cm^{-1} and 2842.06 cm^{-1} while for sugarcane bagasse they are shifted to 1341.47 cm^{-1}, 1603.52 cm^{-1} and 2815.94 cm^{-1}.

The peak at 1598.78 cm^{-1} is known as G-peak. It is a first-order peak which is due to in-plane C-C stretching vibration with E_{2g} symmetry. Its appearance indicates the presence of sp^2 hybridized carbon [**18**]. The peak at 1354.40 cm^{-1} on the other hand is known as D-peak and is also a first-order peak that is only obtained if there is a disorder in the graphitic domain. It is due to the A_{1g} mode in-plane vibration of the graphene sheet. The peak indicates the presence of sp^3 hybridized carbon within a graphitic region [**18**]. The weak and broad peak at 2842.06 cm^{-1} is known as a 2D-peak, which would be strong and narrow for the ordered sample with a large domain size and if the sample is disordered or with small domain size, it becomes weak and broad [**20**]. The full width at half maximum (FWHM) of these peaks (indicated by γ_D, $\gamma_{G,}$ and γ_{2D}) were found to be 208.65 nm, 106 nm and 536.08 nm for mustard oil cake, and 168.04 nm, 76.34 nm and 549.82 nm for sugarcane respectively.

One of the ways to determine the degree of disorder is by calculation of crystallite size which is given by the expression (i) [**20**],

$$\frac{I_D}{I_G} = C\frac{1}{L_a} \qquad \text{(i)}$$

where, C ≈ 4.4 nm wavelength at 514 nm (C-C bond stretching force constant)

L_a= cluster diameter/in-plane correlation length

The peak intensity ratio of mustard oil cake and sugarcane bagasse charcoal was found to be 1.20 and 1.16, which corresponds to crystallite sizes 3.6 nm and 3.79 nm (assuming that the relation holds for laser of wavelength 532 nm).

In conclusion, based on the Raman spectra of the samples, the presence of strong D-peak as well as weak and broad 2D-peak indicates that the pyrolyzed samples contain a significant number of defects with a graphitic domain extending only to the order of a nanometer [**20**].

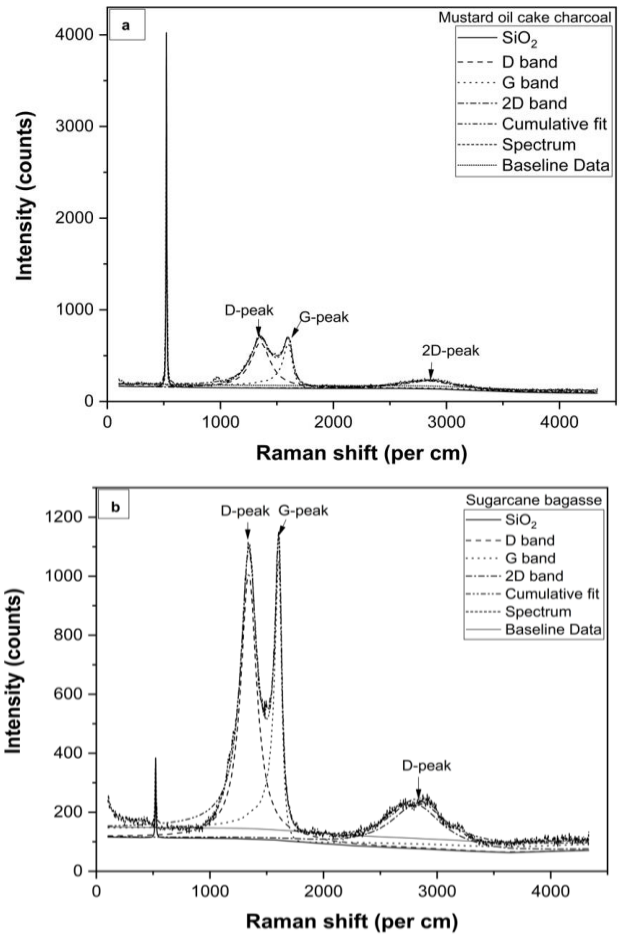

Fig. 2. Raman spectra of charcoal obtained from (a) mustard oil cake and (b) sugarcane bagasse. The experimental peaks are fitted for SiO_2, D, G and 2D bands with appropriate functions as discussed in the text.

Fig. 3 shows the XPS spectra of charcoal prepared by pyrolysis of mustard oil cake and sugarcane bagasse. The survey spectra presented in **Fig. 3(a,b)** consist of the peak of only three elements: carbon, oxygen, and indium (from the sample substrate). The spectra therefore confirm that charcoal contains only carbon and oxygen (also possibly hydrogen as XPS is insensitive to hydrogen and helium). The survey spectra do not show any copper peak indicating non-detectable contamination from the copper plate used to seal the precursor.

To study the chemical states of carbon and oxygen, narrow scan spectra of O1s and C1s were obtained as shown in **Fig. 3(c-f)**. The area under the curve in the narrow scan for different elements (after correcting for instrumental sensitivity) can be used to calculate the relative abundance of the corresponding elements. The sensitivity corrected C:O ratio is found to be 3.77 and 15.17 respectively for mustard oil cake and sugarcane bagasse derived samples.

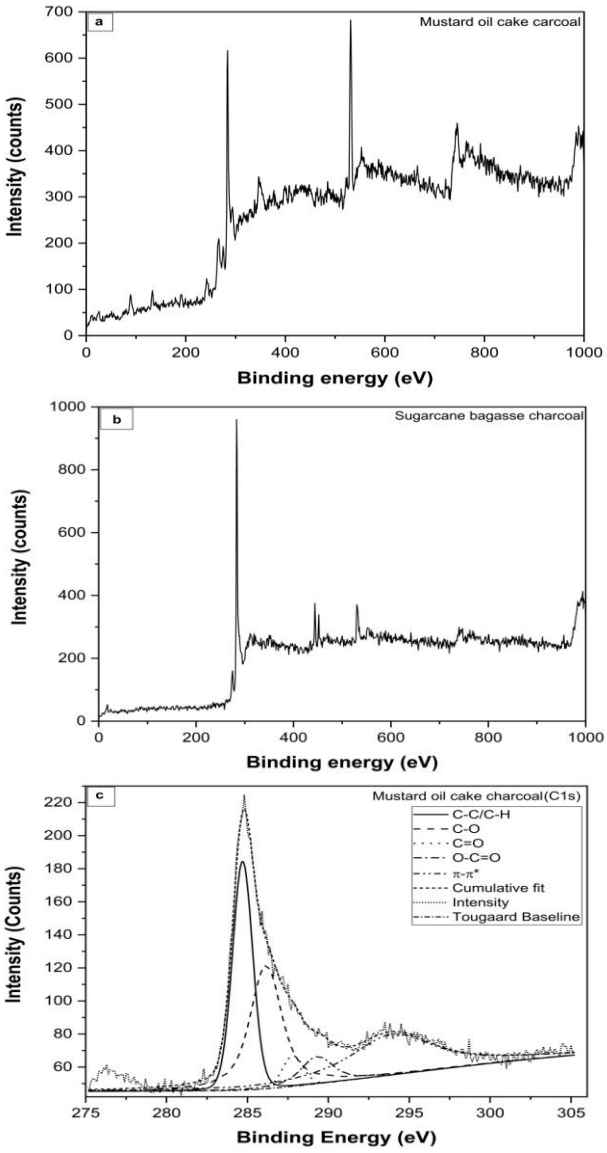

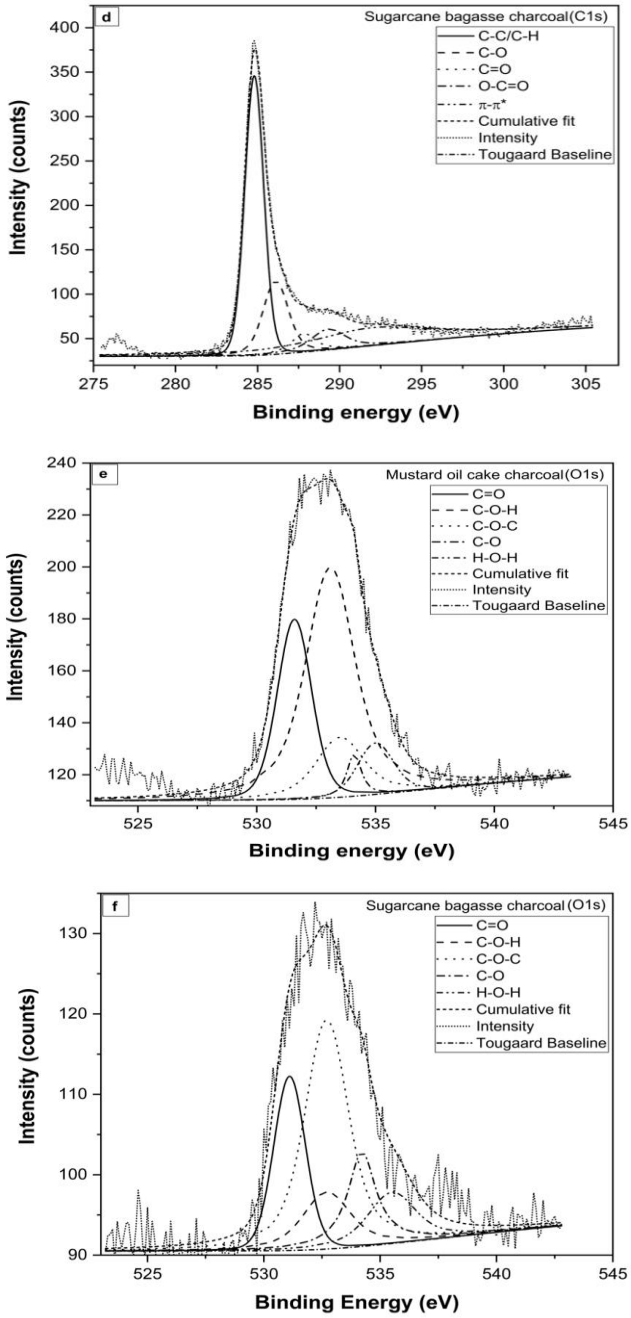

Fig. 3. XPS spectra of the charcoal studied in the current work. (a, b) Survey spectra; (c, d) C1s narrow spectra and (e, f) O1s narrow spectra. The chemical states of oxygen and carbon are fitted with a Voigt function and Tougaard baseline.

This indicates that mustard oil cake-derived charcoal has about three times more oxygen content than that from sugarcane bagasse. In addition, the area of the fitted peak for different chemical states of each element gives their relative abundance [**21**].

Fig. 3(c) and **Fig. 3(d)** show the narrow scan peak of C1s between 275 eV and 305 eV region for charcoal prepared from mustard oil cake and sugarcane bagasse respectively. The experimentally observed peak with maxima between 285 eV and 286 eV can be considered a

cumulation of multiple peaks of different chemical states of carbon such as C ═ O, C ─ O, C ═ O and O ─ C ═ O and C ─ H [**22**]. The peak has a long tail and a shoulder in the higher binding energy region which represents $\pi - \pi^*$ transition. This is a characteristic of the sample with a large number of aromatic rings such as the graphitic system under study. The largest fraction of carbon in the mustard oil cake-derived sample is in the C ─ O state while that in the sugarcane bagasse-derived sample is in the C ─ C/C ─ H state. The relative composition of all the C1s states and their binding energy is tabulated in **Table 1**.

Table 1. The different chemical states of carbon obtained by fitting C1s narrow XPS spectra along with their binding energy and relative composition.

S. No.	Source of Charcoal	Types of bonds	Binding Energy (eV)	Carbon (%)
1	Mustard oil cake	C─ C/ C─H	284.7	30.35
	Sugarcane bagasse		284.79	46.61
2	Mustard oil cake	C─ O	286.14	31.11
	Sugarcane Bagasse		286.1	17.72
3	Mustard oil cake	C ═ O	287.8	4
	Sugarcane Bagasse		287.8	4.97
4	Mustard oil cake	O ─ C ═ O	289.3	6.98
	Sugarcane Bagasse		289.3	7.44
5	Mustard oil cake	$\pi - \pi^*$ transition	293.36	27.53
	Sugarcane Bagasse		292	23.24

O1s narrow spectra in the 520 eV to 545 eV region are presented in **Fig. 3(e)** and **Fig. 3(f)**. In agreement with the C1s spectra, the O1s spectra can also be fitted to the oxygen's chemical states C ═ O, C ─ O ─ C, C ─ O ─ H, C ─ O, and H ─ O ─ H groups [**23**]. The major fraction of oxygen in the mustard oil cake-derived sample is in the C ─ O ─ H state while that from sugarcane bagasse is in C ─ O ─ C state. The full O1s fitting information is indexed in **Table 2**.

Table 2. The different chemical states of oxygen obtained by fitting O1s narrow XPS spectra along with their binding energy and relative composition.

S. No.	Source of Charcoal	Types of bonds	Binding Energy (eV)	Oxygen (%)
1	Mustard oil cake	C ═ O	531.58	24.74
	Sugarcane Bagasse		531.1	20.667
2	Mustard oil cake	C ─ O ─ H	533.09	51.56
	Sugarcane Bagasse		532.7	12
3	Mustard oil cake	C ─ O ─ C	533.5	13.06
	Sugarcane Bagasse		532.7	42.81
4	Mustard oil cake	C ─ O	534.1	3.04
	Sugarcane Bagasse		534.21	13.72
5	Mustard oil cake	H ─ O ─ H	535	41.45
	Sugarcane Bagasse		535.5	10.77

The XPS spectra thus show that the defects in the sample indicated in the Raman spectra originate not only from the amorphous arrangement of carbon atoms in the sample but also from oxygen-related functional groups. These groups disrupt the periodicity in graphitic layers and are a form of defects. Although XPS is not sensitive to hydrogen, the presence of large fractions of C ─ H and O ─ H states of carbon and oxygen suggests sample contains a significant amount of hydrogen atoms.

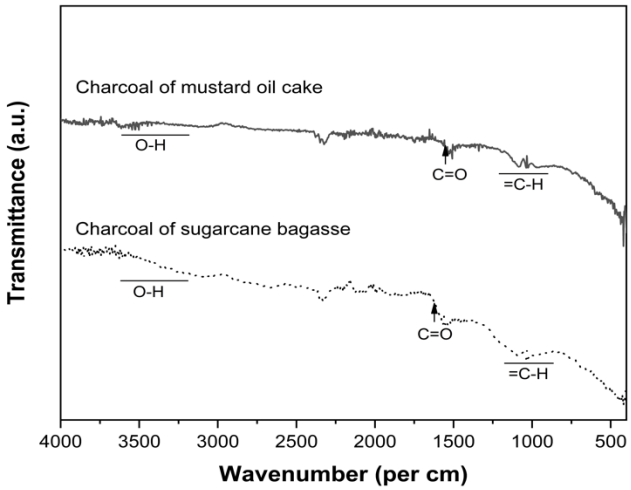

Fig. 4. FTIR spectrum of two different kinds of charcoal prepared in this work as indicated.

Fig. 4 illustrates the FTIR spectra of mustard oil cake and sugarcane. Despite the low signal-to-noise ratio, some significant peaks can be resolved. The broadband in the 3200 – 3650 cm^{-1} is due to O ─ H stretching vibration of the hydroxyl group which indicates the presence of phenol and alcohol groups. The band at 1590 cm^{-1} indicates the presence of the carbonyl group while the broad band at 978 – 1210 cm^{-1} is attributed to vinyl carbon ═ C ─ H [**16,24**].

The FTIR spectra give direct evidence of the presence of hydrogen atoms in the sample which supports the fitting procedure on XPS where hydrogen-containing chemical groups were found to have a large fraction. Moreover, it also further supports the presence of functional groups such as C ─ O, O ─ H, C ─ H, and C ═ O as predicted by XPS spectra of samples.

Morphological analysis of samples

The SEM images displayed in **Fig. 5** depict the morphological features of the charcoal samples derived from sugarcane bagasse and mustard oil cake.

These micrographs presented in **Fig. 5** show a plethora of structural variations, including net-like, plate-like, sheet-like, and occasionally revealing terrace-like features.

Some of the representative features of **Fig. 5** are highlighted in magnified micrographs presented on the right of **Fig. 5**. Particularly, the surface of the sugarcane bagasse charcoal shows the layered and terrace-like features of the lignocellulosic framework preserved in the charcoal even after the strong heat treatment of the original

substance. The high magnification images show an uneven and porous surface structure of the charcoal samples with the size of several micrometers. Similar types of structure have been reported for the charcoal obtained by pyrolysis of green tea and *Butanea monosperma* [**25–28**] targeted towards the development of lithium-ion battery anode and electrode for the doubled-layered capacitor.

Also, relating to the literature works [**29,30**] such porous structures obtained from materials that are otherwise thought of as wastes, could be utilized for preparing novel materials for storage devices and environmental remediation.

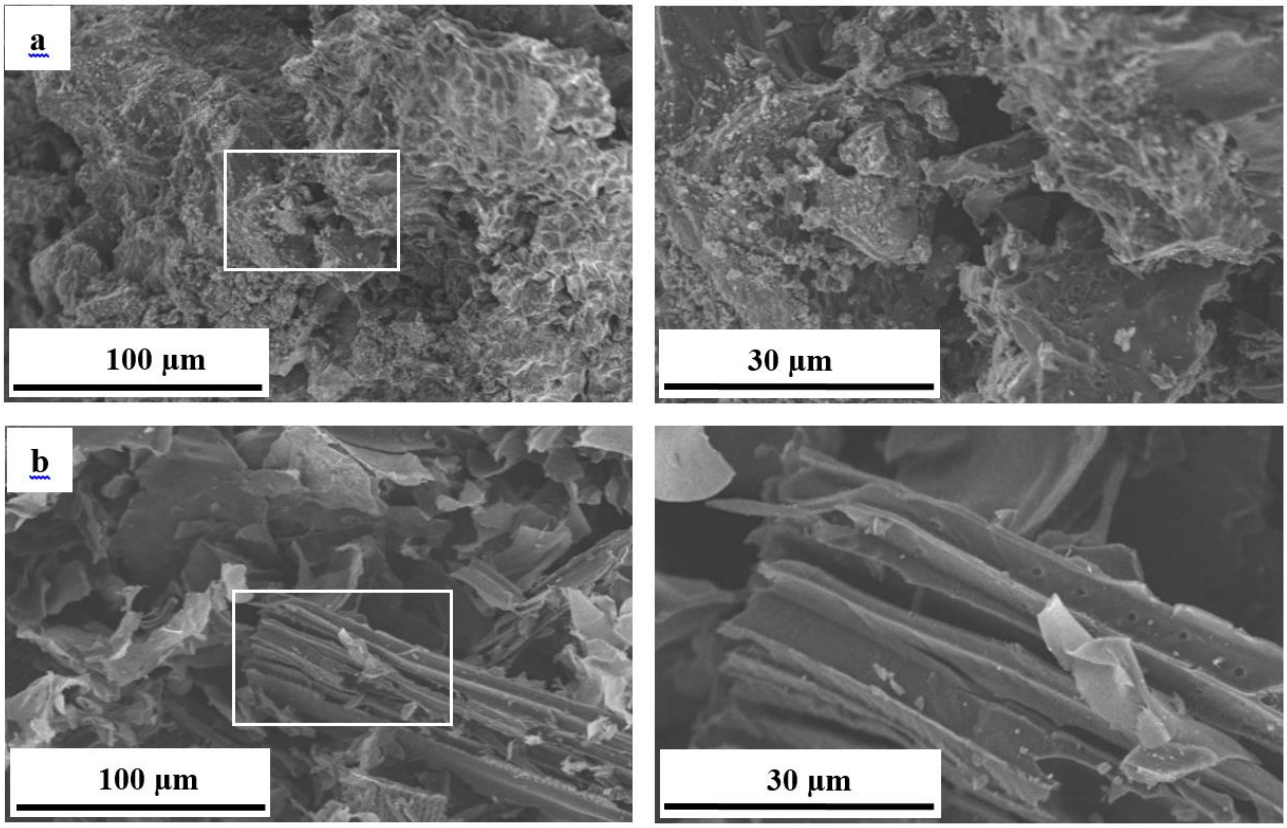

Fig. 5. Lower (left) and higher (right) magnification of scanning electron micrographs of charcoal prepared by pyrolysis of mustard oil cake (a) and sugarcane bagasse (b); the magnifying the areas indicated by white rectangles on respective images on the left.

CONCLUSION

The direct pyrolysis of biomass in the absence of inert gas at high temperatures (for instance 400 °C and higher) is challenging as the non-graphitic carbon starts decomposing around this temperature. However, as the graphitic domains and subsequently functional properties of charcoal generally improve with pyrolysis temperature, methods to pyrolyze biomass in the absence of inert gas are of technological interest. Taking mustard oil cake and sugar cane baggage as examples, it has been demonstrated that direct pyrolysis in a hammer-sealed container can produce charcoal at 900 °C with crystallite size, surface functionality, and morphology comparable to those prepared by conventional methods.

The fact that no copper was detected in XPS indicates that this method does not have contamination issues. Although the sample had a large degree of disorder no nitrogen was present which is a big advantage compared to nitrogen atmosphere synthesis.

Given the sustained scientific and technological interest in the study and use of carbon-based materials, a reduction in the cost of synthesis is always desired. Moreover, the possibility of preparing nitrogen-free carbon in ambient air vastly expands the number of laboratories capable of working on carbon materials. Nevertheless, further research is needed to study the possibilities of using this method to synthesize more ordered forms of carbons as well as to upscale the method to synthesize materials at the gram scale.

ACKNOWLEDGMENTS

We cordially thank the Japanese Ministry of Science and Technology for supporting the research stay of BL at Meijo University, Nagoya, Japan in the frame of "Sakura Science Program 2020". R. A. further gratefully acknowledges the Alexander von Humboldt Foundation for supporting his research stays in Germany.

COMPETING INTERESTS

The authors have no competing interests to declare that are relevant to the content of this article.

FUNDING
No funding was received for conducting this study.

AUTHOR CONTRIBUTIONS
Conceptualization: Ramesh Puri, Bidit Lamsal
Methodology and Formal analysis and investigation: Bidit Lamsal, Deepshikha Karki
Writing - Original draft preparation: Deepsikha Karki
Writing - Review and editing: Bidit Lamsal, Rameshwar Adhikari
Resources: Kamal Prasad Sharma, Takahiro Maruyama
Supervision: Rameshwar Adhikari

DATA AVAILABILITY
The datasets generated during and/or analyzed during the current study are available from the corresponding author upon reasonable request.

REFERENCES

1. H.O. Pierson, Handbook of Carbon, Graphite, Diamonds and Fullerenes: Processing, Properties and Applications, Noyes Publications, **1993**. eBook ISBN: 9780080945903
2. J.J. Manyà, Pyrolysis for Biochar Purposes: A Review to Establish Current Knowledge Gaps and Research Needs, *Environ. Sci. Technol.*, **2012**, 46, 7939–7954. https://doi.org/10.1021/es301029g.
3. A.F. Dias Junior, R.P. Esteves, Á.M. da Silva, A.D. Sousa Júnior, M.P. Oliveira, J.O. Brito, A. Napoli, B.M. Braga, Investigating the pyrolysis temperature to define the use of charcoal, *Eur. J. Wood Wood Prod.*, **2020**, 78, 193–204. https://doi.org/10.1007/s00107-019-01489-6.
4. A. V. Bridgwater, D. Meier, D. Radlein, An overview of fast pyrolysis of biomass, *Org. Geochem.*, **1999**, 30, 1479–1493. https://doi.org/10.1016/S0146-6380(99)00120-5.
5. A.C. Oliveira, A.C.O. De Carneiro, B.R. Vital, W. Almeida, B.L.C. Pereira, M.T. Cardoso, Parâmetros de qualidade da madeira e do carvão vegetal de Eucalyptus pellita F. Muell, *Sci. For. Sci.*, **2010**, 38, 431–439.
6. A.K. Biswas, K. Umeki, W. Yang, W. Blasiak, Change of pyrolysis characteristics and structure of woody biomass due to steam explosion pretreatment, *Fuel Process. Technol.*, **2011**, 92, 1849–1854. https://doi.org/10.1016/j.fuproc.2011.04.038.
7. Y. huan Li, F. min Chang, B. Huang, Y. peng Song, H. yu Zhao, K. jun Wang, Activated carbon preparation from pyrolysis char of sewage sludge and its adsorption performance for organic compounds in sewage, *Fuel*, **2020**, 266. https://doi.org/10.1016/j.fuel.2020.117053.
8. T.R. Bhandari, B. Lamsal, P. Panta, N. Shrestha Pradhan, M. Liebscher, T.B. Katuwal, R. Adhikari, Chemical and Morphological Characterization of Crinis Carbonisatus. *J. Nepal Biotech. Assoc.*, **2024**, 5, 16–22. https://doi.org/10.3126/jnba.v5i1.63742.
9. P.J.F. Harris, Structure of non-graphitising carbons, *Int. Mater. Rev.*, **1997**, 42, 206–218. https://doi.org/10.1179/imr.1997.42.5.206.
10. K. Ishimaru, T. Vystavel, P. Bronsveld, T. Hata, Y. Imamura, J. De Hosson, Diamond and pore structure observed in wood charcoal, *J. Wood Sci.*, **2001**, 47, 414–416. https://doi.org/10.1007/BF00766796.
11. T. Hata, Microstructural investigation of wood charcoal made by spark plasma sintering, *J. Wood Sci.*, **1998**, 44, 332–334. https://doi.org/10.1007/BF00581316.
12. G.R. Surup, M. Foppe, D. Schubert, R. Deike, M. Heidelmann, M.T. Timko, A. Trubetskaya, The effect of feedstock origin and temperature on the structure and reactivity of char from pyrolysis at 1300–2800 °C, *Fuel*, **2019**, 235, 306–316. https://doi.org/10.1016/j.fuel.2018.07.093.
13. A.K. Varma, R. Shankar, P. Mondal, A review on pyrolysis of biomass and the impacts of operating conditions on product yield, quality, and upgradation, *Recent Adv. Biofuels Bioenergy Util.*, **2018**, 227–259. https://doi.org/10.1007/978-981-13-1307-3_10.
14. P. González-García, Activated carbon from lignocellulosics precursors: A review of the synthesis methods, characterization techniques and applications, *Renew. Sustain. Energy Rev.*, **2018**, 82, 1393–1414. https://doi.org/10.1016/j.rser.2017.04.117.
15. M. Morvová, M. Onderka, M. Morvová, I. Morva, V. Chudoba, Pyrolysis of Olive Mill Waste with On-line and Ex-post Analysis, *Waste and Biomass Valorization*, **2019**, 10, 511–520. https://doi.org/10.1007/s12649-017-0126-4.
16. A. Alabadi, S. Razzaque, Y. Yang, S. Chen, B. Tan, Highly porous activated carbon materials from carbonized biomass with high CO2 capturing capacity, *Chem. Eng. J.*, **2015**, 281, 606–612. https://doi.org/10.1016/j.cej.2015.06.032.
17. A. Dufourny, L. Van De Steene, G. Humbert, D. Guibal, L. Martin, J. Blin, Influence of pyrolysis conditions and the nature of the wood on the quality of charcoal as a reducing agent, *J. Anal. Appl. Pyrolysis*, **2019**, 137, 1–13. https://doi.org/10.1016/j.jaap.2018.10.013.
18. Y. Liu, K. Li, Y. Liu, L. Pu, Z. Chen, S. Deng, The high-performance and mechanism of P-doped activated carbon as a catalyst for air-cathode microbial fuel cells, *J. Mater. Chem. A*, **2015**, 3, 21149–21158. https://doi.org/10.1039/c5ta04595a.
19. M.S. Dresselhaus, R. Kalish, J.F. Prins, Ion Implantation in Diamond, Graphite and Related Materials, *Phys. Today*, **1993**, 46, 65–65. https://doi.org/10.1063/1.2808905.
20. R. Escribano, J.J. Sloan, N. Siddique, N. Sze, T. Dudev, Raman spectroscopy of carbon-containing particles, *Vib. Spectrosc.*, **2001**, 26, 179–186. https://doi.org/10.1016/S0924-2031(01)00106-0.
21. G. Greczynski, L. Hultman, X-ray photoelectron spectroscopy: Towards reliable binding energy referencing, *Prog. Mater. Sci.*, **2020**, 107. https://doi.org/10.1016/j.pmatsci.2019.100591.
22. T.R. Gengenbach, G.H. Major, M.R. Linford, C.D. Easton, Practical guides for x-ray photoelectron spectroscopy (XPS): Interpreting the carbon 1s spectrum, *J. Vac. Sci. Technol. A Vacuum, Surfaces, Film*, **2021**, 39. https://doi.org/10.1116/6.0000682.
23. L. Stobinski, B. Lesiak, A. Malolepszy, M. Mazurkiewicz, B. Mierzwa, J. Zemek, P. Jiricek, I. Bieloshapka, Graphene oxide and reduced graphene oxide studied by the XRD, TEM and electron spectroscopy methods, *J. Electron Spectros. Relat. Phenomena*, **2014**, 195, 145–154. https://doi.org/10.1016/j.elspec.2014.07.003.
24. J.F. González, S. Román, C.M. González-García, J.M.V. Nabais, A.L. Ortiz, Porosity development in activated carbons prepared from walnut shells by carbon dioxide or steam activation, *Ind. Eng. Chem. Res.*, **2009**, 48, 7474–7481. https://doi.org/10.1021/ie801848x.
25. S. Ahmed, A. Ahmed, M. Rafat, Investigation on activated carbon derived from biomass Butnea monosperma and its application as a high performance supercapacitor electrode, *J. Energy Storage*, **2019**, 26, 100988. https://doi.org/10.1016/j.est.2019.100988.
26. S.W. Han, D.W. Jung, J.H. Jeong, E.S. Oh, Effect of pyrolysis temperature on carbon obtained from green tea biomass for superior lithium ion battery anodes, *Chem. Eng. J.*, **2014**, 254, 597–604. https://doi.org/10.1016/j.cej.2014.06.021.
27. D. Wang, Z. Geng, B. Li, C. Zhang, High performance electrode materials for electric double-layer capacitors based on biomass-derived activated carbons, *Electrochim. Acta*, **2015**, 173, 377–384. https://doi.org/10.1016/j.electacta.2015.05.080.
28. J. Han, L. Zhang, B. Zhao, L. Qin, Y. Wang, F. Xing, The N-doped activated carbon derived from sugarcane bagasse for CO2 adsorption, *Ind. Crops Prod.*, **2019**, 128, 290–297. https://doi.org/10.1016/j.indcrop.2018.11.028.
29. L.K. Shrestha, R.G. Shrestha, S. Maji, B.P. Pokharel, R. Rajbhandari, R.L. Shrestha, R.R. Pradhananga, J.P. Hill, K. Ariga, High surface area Nanoporous graphitic carbon materials derived from Lapsi seed with enhanced supercapacitance, *Nanomaterials*, **2020**, 10. https://doi.org/10.3390/nano10040728.
30. R. Rajbhandari, L.K. Shrestha, R.R. Pradhananga, Preparation of Activated Carbon from Lapsi Seed Stone and its Application for the Removal of Arsenic from Water, *J. Inst. Eng.*, **1970**, 8, 211–218. https://doi.org/10.3126/jie.v8i1-2.5113.

GRAPHICAL ABSTRACT

Schematic diagram showing the preparation and structural characterization of the charcoal by direct pyrolysis method